Spontaneous selective epitaxial growth of compositionally modulated AlGaAs with an orientation-dependent band gap

Michael E. Hoenk, Kerry J. Vahala

Michael E. Hoenk, Kerry J. Vahala, "Spontaneous selective epitaxial growth of compositionally modulated AlGaAs with an orientation-dependent band gap," Proc. SPIE 1285, Growth of Semiconductor Structures and High-Tc Thin Films on Semiconductors, (1 October 1990); doi: 10.1117/12.20819

SPIE.

Event: Advances in Semiconductors and Superconductors: Physics Toward Devices Applications, 1990, San Diego, CA, United States

Invited Paper

Spontaneous selective epitaxial growth of compositionally modulated AlGaAs with an orientation dependent bandgap

Michael E. Hoenk and Kerry J. Vahala

Thomas J. Watson, Sr., Laboratories of Applied Physics
California Institute of Technology, 128-95, Pasadena, CA 91125

Abstract

We have demonstrated selective epitaxial growth of $Al_xGa_{1-x}As$, with an abrupt transition in the bandgap lateral to the growth direction. Spontaneous compositional modulation, with an associated reduction in the effective bandgap, occurs in AlGaAs grown by molecular beam epitaxy on the sides of grooves in a GaAs substrate. The bandgap is observed to be dependent on the groove orientation. Possible mechanisms for the orientation dependent growth are discussed.

1 Introduction

In semiconductor crystals, the deBroglie wavelength of an electron is several nanometers in extent. Consequently, quantum size effects dominate the behavior of electrons in structures with one or more dimensions on the nanometer scale. Such structures, fabricated using planar growth technology (e.g., MBE, OMVPE), have found application in a wide range of devices. Fabrication of higher dimensional nanometer scale structures presents an interesting challenge, because of important consequences for devices [1]. There have been a variety of approaches to solving this difficult problem. *In situ* growth of nanometer scale structures is an attractive alternative, because fabrication is accomplished in a single growth step (including growth of the surrounding heterostructure), and there is no fabrication induced damage to the structures. Several techniques have been used to fabricate higher dimensional nanometer scale structures *in situ* [2,3,4,5]. While no technique has emerged which solves all of the problems in nanofabrication, progress has been remarkable, and there are strong indications that useful applications will arise in the near future. For example, stimulated emission was recently demonstrated in quantum wire lasers, using growth on a patterned substrate [2].

In this paper, we present a novel method for the selective growth of nanometer scale structures *in situ* [6]. The technique is called orientation selective epitaxy (OSE). In sections 2 and 4, experimental data are presented, illustrating the nature of OSE growth on grooves in a (100) GaAs substrate. In section 3, we propose a model for orientation selective epitaxy, and discuss implications of the model.

2 Orientation selective epitaxy: Growth in a $[01\bar{1}]$ groove

In this section, we present the initial observations of orientation selective epitaxy [6]. Cathodoluminescence and transmission electron microscopy are used to analyze the electronic and structural properties of AlGaAs grown in

grooves on a patterned substrate. We find that AlGaAs grown on the sides of grooves parallel to [01$\bar{1}$] contains a superlattice, oriented approximately along the (111)Ga direction.

2.1 Sample preparation: MBE 815

Grooves parallel to the [01$\bar{1}$] direction were etched into a (100)GaAs substrate, using standard photolithography and wet etching techniques. The etch, using a 3:1:40 mixture of $H_3PO_4 : H_2O_2 : H_2O$, produced grooves approximately $15\mu m$ wide and $5\mu m$ deep. Growth of the epilayers was done in a Riber 2300 molecular beam epitaxy machine, at a substrate temperature of $600°C$. The substrate was rotated at 48 rpm during the growth. The structure of the epilayers is as follows: (1.) 1 μm GaAs buffer layer, (2.) 1 μm $Al_{0.25}Ga_{0.75}As$ layer, (3.) 100 Å GaAs quantum well, and (4.) 1000 Å $Al_{0.25}Ga_{0.75}As$ cap layer. All layers are undoped. Any influence of the quantum well on the luminescence properties of the sample was ruled out by cathodoluminescence measurements on a sample in which the quantum well had been removed with a wet chemical etch. The azimuthal angle of the gallium cell was 33.2°. The azimuthal angle of the aluminum cell was 42.0°. The angular separation of the gallium and aluminum cells, in the projection onto the (100) plane, was 65.0°.

2.2 Cathodoluminescence

Cathodoluminescence scanning electron microscopy [7] reveals a correlation between the facet orientation and the composition of AlGaAs epilayers in the grooves. Figure 1 shows spectrally resolved cathodoluminescence images taken of a cross section of a groove at two different wavelengths. The AlGaAs grown on the sides of the groove luminesces at a different wavelength than AlGaAs grown on other facets in the sample. Cathodoluminescence spectra show that the peak luminescence from the sides of the groove occurs at 7160 Å. Compared to the 6670 Å luminescence from AlGaAs grown on the bottom of the groove and on the unpatterned (100) substrate, this corresponds to a $127meV$ reduction in the band gap of material grown on the sides of the groove. Spectra taken from points near the boundary between the side and bottom facets of the groove show two distinct emission peaks, indicating that the band gap changes abruptly at the interface. The spatial resolution of cathodoluminescence, which is on the order of a micron in GaAs, is insufficient to determine the length scale on which the compositional transition takes place. In order to determine this, transmission electron microscopy was performed on a cross section of a groove.

2.3 Transmission electron microscopy

Using transmission electron microscopy, we were able to study the variation of aluminum concentration in the groove, with a spatial resolution of approximately 10 Å [8]. The sample was prepared for cross sectional transmission electron microscopy using the standard techniques of mechanical thinning and argon ion milling. Dark field imaging of the sample was done with a Philips EM430 transmission electron microscope, using the (200) diffracted beam. We observe quasi-periodic modulation in the composition of AlGaAs grown on the side of the groove (figure 2). The compositional modulation occurs in the side facets of the groove, which are misoriented (111)Ga facets. Within the limits of experimental error, the modulation occurs along the [111] direction. The layers are not perfectly straight, nor is the modulation perfectly periodic. The period of the compositional modulation is approximately 70 Å. On the the adjacent (811) and (411) facets, the AlGaAs composition is observed to be uniform. At the interface between these facets and the (111) facet, we observe an abrupt transition from uniform to compositionally modulated AlGaAs (figure 3). This compositional modulation is unique, because it occurs selectively on the side facets of the groove, and the abrupt termination at the facet boundary constitutes a heterojunction lateral to the growth direction. Henceforth, this structure will be referred to as an orientation selective epitaxy superlattice, or OSE superlattice.

The period of the OSE superlattice is not correlated with the period of rotation of the substrate. From measurements of the growth rate and the substrate rotation rate, approximately 3-5 Å of AlGaAs were deposited in the time required for one rotation of the sample holder, depending on the facet orientation. This is approximately the

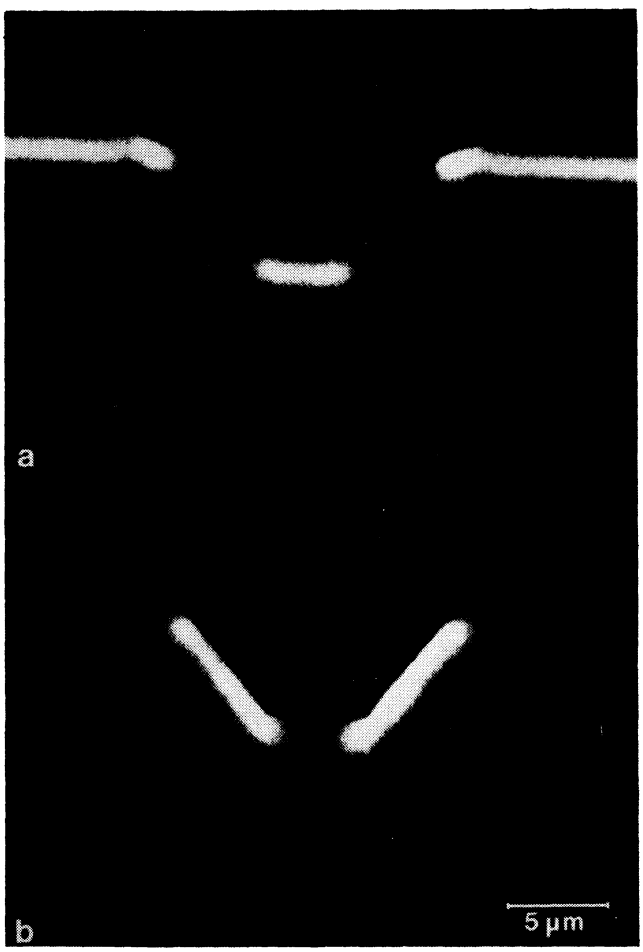

Figure 1: Spectrally resolved cathodoluminescence micrographs of a cross section of a groove in sample MBE 815. The substrate is in the bottom part of each micrograph, and the AlGaAs layers form a narrow band on top of the substrate, following the contour of the groove. Micrograph 'a' shows AlGaAs luminescence at 6700 Å, and micrograph 'b' shows AlGaAs luminescence at 7000 Å. The AlGaAs on the sides of the groove luminesces at a longer wavelength than AlGaAs grown on other surface orientations, indicating that the composition of AlGaAs depends on the facet orientation.

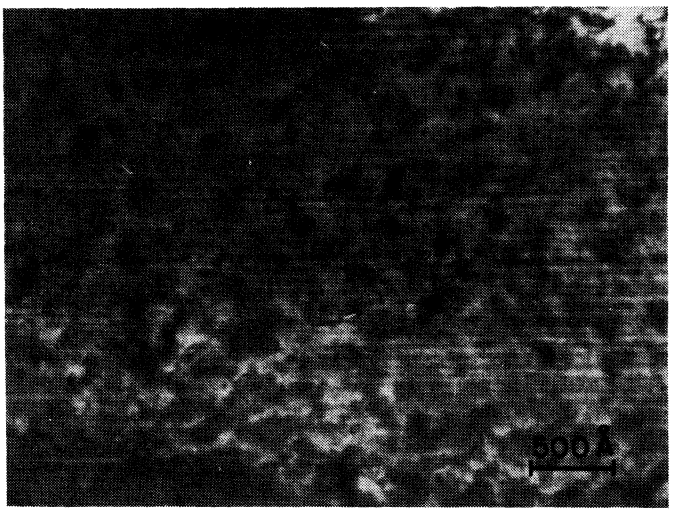

Figure 2: Dark field transmission electron micrograph showing the cross section of AlGaAs grown on the side facet of a groove, using the (200) reflection. The quasi-periodic contrast corresponds to an OSE superlattice (see text), with a period of 70 Å. The [111] direction is vertical in the micrograph.

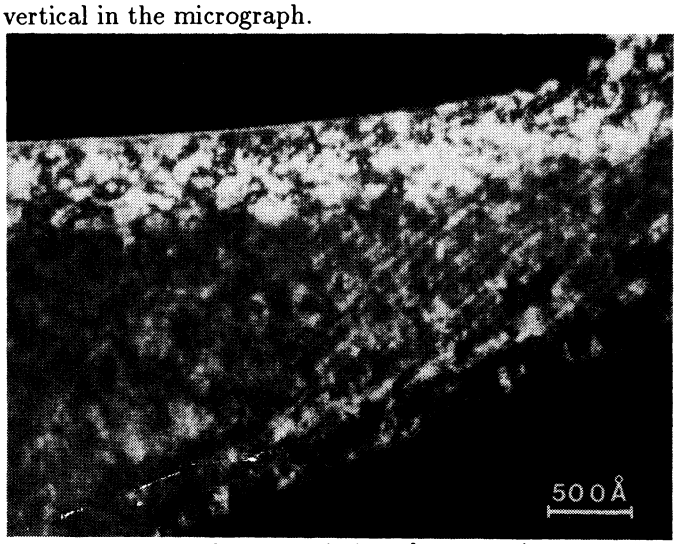

Figure 3: Dark field transmission electron micrograph of a cross section of the groove, showing the interface between the side and bottom facets. The left half of the micrograph shows AlGaAs grown on the bottom of the groove. The right half, in which compositional modulation is seen along the [111] direction, shows AlGaAs grown on the side of the groove. The compositional modulation terminates abruptly at the facet interface.

thickness of a single monolayer of growth. The significance of the correspondence between the monolayer growth time and the period of rotation will be discussed in section 3.

Transmission electron microscopy was done on another growth to verify the existence of a superlattice on the sides of $[01\bar{1}]$ grooves. The growth was done under the same conditions as were described above, and the results confirm the observations presented in this paper. In this sample, images of the substrate-epilayer interface show that the superlattice is inclined with respect to the growth direction by a few degrees. The modulation was associated with a reduction in the band gap observed by cathodoluminescence. Transmission electron microscopy of a sample grown at $700°C$ did not reveal compositional modulation. This indicates that orientation selective epitaxy is sensitive to the growth conditions, as well as the facet orientation.

2.4 Determination of the OSE superlattice parameters

The shifts in the cathodoluminescence emission from the sides of grooves are associated with the presence of the OSE superlattice, observed by transmission electron microscopy. Other groups have found a similar reduction of the effective bandgap due to compositional modulation in an alloy [9,10,11,12], indicating that the cathodoluminescence data are consistent with the existence of the OSE superlattice. However, a red shift in the luminescence peak is also consistent with a reduction in the average aluminum concentration, which could occur due to surface migration of Ga during growth [13]. In order to determine the average aluminum concentration in the OSE superlattice, a zinc diffusion was used to disorder the compositional modulation. The sample was sealed in an evacuated quartz ampoule with $ZnAs_2$ powder, and placed in a 650 $°C$ furnace for one hour. Following the diffusion, cathodoluminescence spectra taken at $77K$ showed that the emission peak occurred at 6920 Å throughout the sample. A similar diffusion, done at 600 $°C$ for one hour, resulted in only partial disordering of the compositional modulation. This indicates that the average aluminum concentration in the OSE superlattice is the same as the aluminum concentration in the uniform alloy grown on the unpatterned (100) substrate, and the shift in the cathodoluminescence peak is caused by compositional modulation about the nominal aluminum concentration, $x \approx 0.25$.

The transmission electron micrographs do not give quantitative information about the modulation amplitude in the OSE superlattice. Given the Zn diffusion results of section 2.4, we can infer from the cathodoluminescence data that the average aluminum concentration is 0.25, with a minimum concentration less than or equal to 0.17. This upper limit is not an accurate estimate, because the observed period of the OSE superlattice, 70 Å, indicates that the position of the luminescence peak will be strongly influenced by quantum size effects. A first order calculation, based on a Kronig Penney model of the potential, indicates that the minimum aluminum concentration in the superlattice is less than 0.1, and the amplitude of the modulation in aluminum concentration is larger than 0.3.

2.5 Discussion

Previous observations of spontaneous compositional modulation and ordering in AlGaAs have been limited to growth on (110) and (100) GaAs substrates [14,15,16]. In all cases, the modulation was observed to occur along the growth direction. Our observation of compositional modulation occurring spontaneously in growth on a (111) surface is new for the $Al_xGa_{1-x}As$ alloy.

The OSE superlattice bears some similarity to tilted superlattices grown on vicinal substrates [5,17]. However, there are several significant differences between tilted superlattices and OSE superlattices. First, the direction of growth is different. Second, the growth of tilted superlattices requires the use of alternating beam growth, which involves periodic shuttering of atomic and molecular fluxes. Finally, the OSE superlattice is grown selectively on particular facets in the grooves, whereas tilted superlattices are grown on planar vicinal substrates. Despite these differences, the mechanisms responsible for alloy segregation in the two cases may be similar. This is discussed in section 3.

The spatially abrupt change in composition, from uniform AlGaAs to an OSE superlattice, effectively forms a heterojunction lateral to the growth direction. This is the first such structure which occurs spontaneously during the growth. These results suggest that growth on a patterned substrate may be useful for the *in situ* growth of higher dimensional nanometer scale structures. In the following sections, the phenomenon of orientation selective epitaxy is considered in more detail.

3 Model for orientation selective epitaxy

In this section, a model for orientation selective epitaxy will be discussed. The model considers the geometry of the MBE growth chamber and the effect of substrate rotation on the group III fluxes, but does not taken into account several phenomena which affect the detailed dependence of the composition on surface orientation (e.g., the effects of chemistry, surface reconstruction, and bond geometry for different facets). It will be shown that there is a connection between orientation selective epitaxy and the growth of tilted superlattices by migration enhanced epitaxy [17]. This connection is based on the effect of the surface orientation in a patterned substrate on the fluxes of molecules arriving at the surface. The implications of the model will be discussed, and related to the experiments presented in this paper.

3.1 Growth of AlGaAs with time dependent fluxes

In section 2.5, the similarity between OSE superlattices and tilted superlattices [17] was mentioned. Tilted superlattices are grown on vicinal surfaces, using alternate deposition of a fraction of a monolayer of GaAs and a fraction of a monolayer of AlAs to create modulation of the AlGaAs composition in the growth plane. In-plane compositional modulation occurs when nucleation and growth takes place via addition of atoms to steps in the surface (i.e., growth by step flow). Growth by step flow is promoted by alternate deposition of the group III and group V elements, in order to take advantage of enhanced surface migration of gallium and aluminum in the absence of an arsenic flux.

We propose that the OSE superlattices observed in our experiments result from growth by step flow on facets which are inclined with respect to the rotation axis of the substrate. In the next section, we will show how this can occur.

3.2 Orientation selective epitaxy and the OSE superlattice: Selective migration enhanced epitaxy

If the growth proceeds strictly by step flow, the entire growth can be viewed as the propagation of individual steps, and it is the in-plane variation of the composition which determines the spatial dependence of the composition in the resulting crystal. In this section, we will discuss the effect of substrate rotation on the in-plane composition in growth by MBE on a patterned substrate.

For facets which are inclined with respect to the rotation axis, rotation of the substrate results in time dependence of the fluxes. Furthermore, there is a phase difference in the deposition of gallium and aluminum during growth on these facets, due to the angular separation of the effusion cells in the MBE growth chamber. The orientations of the effusion cells for the two experiments are given in sections 2.1 and 4.1. The nominal aluminum fraction was 0.25. Given these parameters, we can calculate the fluxes as a function of time for a given facet orientation. Residual As flux during the group III deposition should not have a significant effect on the formation of an OSE superlattice, because Gaines et al. found that leaving the group V flux on during the group III deposition did not have a measurable effect on the growth of tilted superlattices [17].

Assuming that the growth occurs by step flow, the phase difference in the deposition of gallium and aluminum

will result in a significant in-plane variation of the aluminum fraction. By integrating the fluxes, we can calculate the average aluminum concentration for successive columns of atoms added to a step during the growth of a monolayer, for a given terrace width. Using the parameters in the growths discussed in section 4, we find that, for ideal growth by step flow on a (111) facet, the composition of the layer will have a large in-plane variation, with an amplitude which is nearly independent of terrace width (see figure 4). For this facet, the aluminum concentration varies by more than 0.5 in the plane of growth, for idealized step flow growth. Stacking of successive layers forms an OSE superlattice. The angle between the OSE superlattice planes and the substrate is determined by the relationship between the rotation rate and the (orientation dependent) monolayer growth rate. The quality of the OSE superlattice is determined by effects not considered by this simple model, such as thermally induced roughness of the step edges and island formation on the terraces.

The expected in-plane variation of the aluminum concentration depends on the relative orientation of the group III effusion cells, the facet orientation, and the orientation of the group V cell. For facets which are not as highly inclined with respect to the (100) surface as the (111) facet, the amplitude of the OSE superlattice would be correspondingly lower. Calculation of the expected amplitude for the (211) facet, for the same conditions used for the (111) facet, gives a composition which varies from 0.18 to 0.33, within a 20 column terrace width. The amplitude may be further reduced, because the smaller modulation of the arsenic flux will reduce the mobility of adatoms on the (211) facet. However, near a local perturbation in the surface orientation, there may be an enhancement of the OSE superlattice in the shadow of the perturbation. This is a possible explanation for the observed enhancement of the compositional modulation in the (211) facet of NSI2, near small (111) facets (see section 4).

3.3 Discussion of the model

To summarize, this model is equivalent to a prescription for selective migration enhanced epitaxy. The time dependence of the fluxes arises from rotation of the substrate during growth, and inclination of the surface with respect to the rotation axis. If the growth occurs by step flow, in-plane variation of the composition can occur on the inclined facets, resulting in the selective growth of a superlattice tilted with respect to the substrate orientation. The amplitude of the compositional modulation, for ideal step flow growth, is determined by the orientation of the surface with respect to the rotation axis, and the geometry of the MBE growth chamber. The angle between the substrate and the superlattice is determined by the relationship between the rotation rate and the (facet dependent) growth rate.

The geometrical dependence of OSE superlattice growth suggests methods for optimization and manipulation. Increasing the angular separation of the group III cells would increase the expected amplitude of the OSE superlattice. The use of larger azimuthal angles for the effusion cells would extend the range of facet orientations which would exhibit an OSE superlattice. The tilt angle of the OSE superlattice could be varied by adjusting the rate of substrate rotation. This suggests a technique for fabricating a two dimensional array of quantum wires. By periodically varying the rotation rate, the OSE superlattice could be sharply bent at regular intervals, in such a way as to provide two dimensional confinement of electrons and holes. More sophisticated variation of the rotation rate might provide a complicated variation of the composition in two dimensions. It should be possible to grow an OSE superlattice on an unpatterned substrate, by tilting the substrate with respect to the rotation axis. Finally, the assumptions of this model are not specific to the growth of AlGaAs on patterned substrates. Therefore, it should be possible to apply this technique to other material systems.

The model implies that the period of the superlattice is related to the terrace width on the patterned substrate. This suggests that it would be interesting to study the dependence of OSE growth on groove orientation. In addition, the superlattice should be tilted with respect to the growth direction. These issues are addressed in section 4.

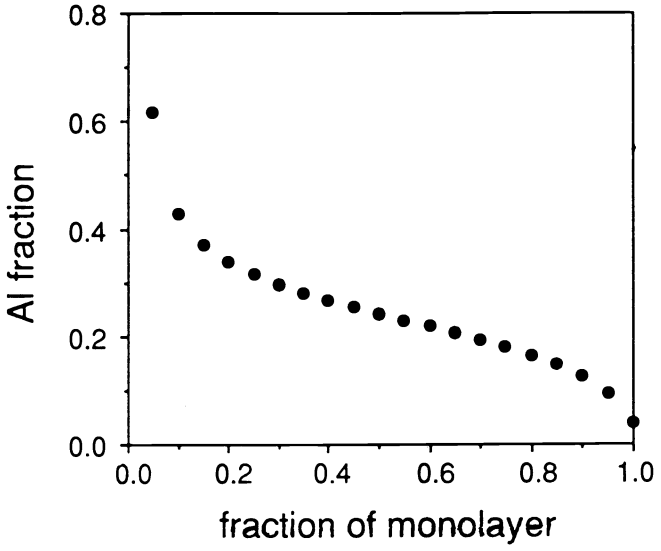

Figure 4: Calculated variation of the composition of columns of atoms added to steps in a (111) facet, with terraces 20 atoms wide, assuming ideal growth by step flow. The growth chamber geometry is described in the text. The aluminum fraction varies by more than 0.5 in the plane of growth.

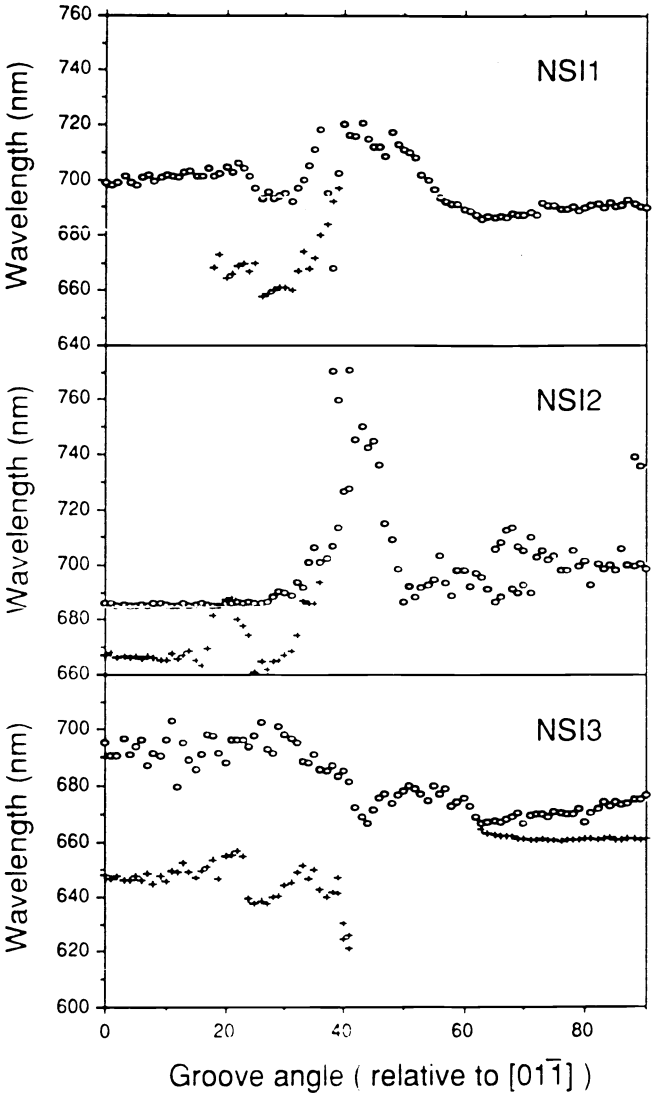

Figure 5: Plot of the AlGaAs peak as a function of groove orientation, relative to the [01$\bar{1}$] groove, for NSI1, NSI2, and NSI3. The circles represent luminescence from the side of the grooves, and the '+' symbols represent luminescence from an additional facet at the top of the groove.

4 Orientation selective epitaxy: Variation of groove orientation

Three new growths will be discussed in this section, NSI1, NSI2, and NSI3. The geometry and conditions in the growth of MBE 815, discussed in section 2, are most closely duplicated in NSI1. The relative orientations of the effusion cells are similar, the layer thicknesses are the same, and the growth rate has been adjusted so that the ratio of the growth rate to substrate rotation rate is roughly the same as for MBE 815. Measurements on the new samples confirm the results from MBE 815, and provide additional information on the nature of OSE growth.

4.1 Sample preparation: NSI1, NSI2, and NSI3

In order to study in detail the dependence of orientation selective epitaxy on the groove orientation, we prepared substrates with grooves varying in orientation between $[01\bar{1}]$ and [011]. The substrates were patterned using the same procedure outlined in section 2. Growth of the epilayers was done in a Varian GEN II molecular beam epitaxy machine, with a substrate temperature of $600°C$. The $Al_{0.25}Ga_{0.75}As$ growth rate was 0.88 $\mu m/hr$. The growth of sample NSI1 consists of a 1 μm GaAs buffer layer, followed by a 1 μm $Al_{0.25}Ga_{0.75}As$ layer. Samples NSI2 and NSI3 consist of a 0.5 μm GaAs buffer layer, followed by 0.5 μm $Al_{0.25}Ga_{0.75}As$. In these growths, the gallium and aluminum cells were separated by $\frac{\pi}{4} radians$, in the projection onto the (100) plane. All layers were undoped.

4.2 Orientation considerations

As the angle of the groove, relative to the $[01\bar{1}]$ groove, changes from 0° to 90°, the facets exposed by the chemical etch change orientation. The facets which appear depend on the chemical etchant, and on the conditions and duration of the etch. Because selective etches tend to cause pitting of the surface, the etchant which we have chosen is a slow, non-selective etch. The cross section of grooves oriented near 0° and 90° had a flattened 'V' shape, with straight sides and a flat bottom. This is a similar profile to that observed in the growths of section 2. Grooves oriented near 45° had a more rounded profile, with a gradual transition between the side and bottom of the grooves.

The growths exhibit some variation of the surface morphology in the grooves, and in luminescence characteristics. The differences in the morphology of the three samples, and the differences in luminescence characteristics, may be due to variation in either the etch conditions or the MBE growth conditions. Orientation selective epitaxy is sensitive to the surface profile in the groove, which may in turn depend upon the conditions of the etch. In particular, small misorientations can have a significant effect on the quality of epitaxial growth on a {110} surface [18]. The etch rate is quite sensitive to the concentration of H_2O_2, which changes as the etchant ages. Uncertainty in adjusting the substrate temperature and growth rate in MBE may result in variation of the growth conditions for the samples studied.

4.3 Cathodoluminescence: Dependence on surface orientation

We characterized the cathodoluminescence emission as a function of groove angle in the three samples. Cathodoluminescence scanning electron microscopy of these samples reveals a dependence of the peak AlGaAs emission on surface orientation. The position of the cathodoluminescence peak, as a function of groove angle, is shown in figure 5. The epitaxial layers luminesce strongly, indicating that the quality of the growth is good. The position of the luminescence peaks are to be compared to the luminescence peak from the unpatterned (100) AlGaAs, which occurs at $669nm$ for NSI1, $672nm$ for NSI2, and $663nm$ for NSI3. Emission from the sides of the grooves is, in general, considerably stronger than emission from the unpatterned (100) AlGaAs epilayers. Red shifts, relative to the luminescence from these unpatterned regions, are observed on the side facets of most groove orientations. The largest shifts, and the strongest luminescence, are observed in the grooves between 40° and 45°. In addition, some grooves exhibit strong blue shifts in NSI3.

For all three samples, the position of the luminescence peak is nearly independent of groove orientation from 0° to 20°, and from 70° to 90°. Between 20° and 60°, the position of the luminescence peak depends on the groove orientation. The samples exhibit different faceting characteristics in this range of angles. Samples NSI1 and NSI2, in which the faceting is similar, have a similar dependence of the luminescence on groove angle. Sample NSI3 has both different faceting behavior and different luminescence characteristics.

Monotonic dependence of the bandgap on groove orientation is observed in some ranges of surface orientation. For the side facets, NSI1 shows a shift in the luminescence peak from $687nm$ in the 62° groove, to $717nm$ in the 48° groove. The surface morphology in this range of groove angles is very good. Similarly, NSI2 exhibits a dramatic shift in the luminescence peak for grooves between 50° and 45°. In the 50° groove, the peak occurs at $687nm$, and in the 45° groove, the peak has shifted to $745nm$. This represents a difference of 140 meV in the effective bandgap for a mere 5° change in groove angle. Grooves in the range 46°-55° have good surface morphology, but at 45° some faceting is evident.

Sample NSI3 has a much smaller dependence of the luminescence peak on groove angle in this range. As indicated by the lack of faceting characteristic of growth on misoriented (110) surfaces, which was observed in NSI1 and NSI2, this is most likely due to a different groove profile in sample NSI3.

The top facet, which is distinct from the side facet in grooves from 0° to approximately 40°, also exhibits a strong dependence of the bandgap on groove orientation. Again, NSI1 and NSI2 are similar, while NSI3 has markedly different properties. In the 30° groove of NSI1, the top facet has its peak luminescence at $660nm$. As the groove angle changes toward 39°, the luminescence peak shifts to $697nm$. In NSI2, from the 27° to the 33° grooves, the luminescence peak shifts from $662nm$ to $687nm$. In NSI3, the top facet first appears in the 41° groove, where it has a luminescence peak at $621nm$. Compared to the $663nm$ peak of AlGaAs grown on unpatterned regions of this sample, this is the strongest blue shift observed in any of the growths. From the 41° to the 35° grooves, the luminescence shifts to $650nm$. Between 35° and 25°, the peak shifts toward $638nm$.

Significant scatter in the position of the luminescence peak is associated with rough surfaces and/or faceting in the corresponding grooves. This is the case, for example, for grooves between 25° and 45° in NSI1 and NSI2, between 60° and 90° in NSI2, and between 0° and 20° in NSI3. The origin of different surface morphology of the three samples is discussed in section 4.2. Faceting of growth is particularly important to consider in orientation selective epitaxy. In addition to the dependence of orientation selective epitaxy on the azimuthal angle of the surface normal (see section 3), the chemistry on different facet orientations may affect the composition, and interfacet diffusion may affect the relative compositions of adjacent areas in the growth. Luminescence from a faceted surface is expected to be dominated by the facets with the lowest bandgap. In our cathodoluminescence measurements, differences in the surface morphology are associated with different luminescence characteristics. This association can be dramatic, as in the case of diagonal facets crossing the sides of the grooves in samples NSI1 and NSI2, for grooves between 35° and 45°. Such facets can have emission peaks red shifted by as much as 1000 Å, relative to luminescence from AlGaAs grown on the unpatterned (100) substrate.

4.4 Transmission electron microscopy

Transmission electron microscopy was used to look at the composition of the samples NSI1, NSI2, and NSI3. The sample preparation and diffraction conditions are described in section 2.3. Because of considerations of sample preparation and imaging in the microscope, only grooves oriented roughly along the $[01\bar{1}]$ and [010] directions were studied. The results of the TEM measurements confirm the results obtained for MBE 815. Two new results will be discussed in this section.

The side facets of $[01\bar{1}]$ grooves in NSI2 are observed to consist of a wide (211) facet, and a narrow (111) facet next to the bottom of the groove. Strong compositional modulation is observed on the (111) facet, similar to that observed in MBE 815. The (211) facet shows some interesting features, which were mentioned briefly in section 3. Compositional modulation in other samples has been observed to intersect the substrate/epilayer interface, but at a

relatively shallow angle. In the (211) facet, there is a 22° angle between the planes of compositional modulation and the substrate/epilayer interface (see figure 6). Furthermore, the contrast is observed to be stronger for compositional modulation in the vicinity of small (111) facets in the surface. A possible explanation for this enhancement of the modulation, based on the model discussed in section 3, is that the amplitude of the rotation-induced flux modulation is larger near the (111) facets, due to locally enhanced shadowing of the fluxes.

In the side facet of a groove oriented approximately along [010], we observe quantum wire-like structures with very strong contrast, with a width of approximately 60 Å(see figure 7). Narrow bright bands, oriented approximately parallel to the (101) facet, run through the epilayers. The bands are continuous for length scales of up to a micron, and they appear to terminate at perturbations, or small facets, in the substrate/epilayer interface and the surface. The contrast indicates that these bands are aluminum rich, but their origin is unknown. Wire-like structures are observed as an array of Ga-rich and Al-rich layers, which are terminated by the narrow Al-rich layers. The phase between wire structures in adjacent bands is different for different bands. Some of the wire structures exhibit very strong contrast.

In the bottom of the groove, and in AlGaAs grown on unpatterned (100)GaAs, we observe a weak superlattice, which is due to an external modulation of the fluxes. The external modulation is attributed to a small fluctuation in the temperature of the group III effusion cells. The period of the external modulation is short (approximately 25 Å on the bottom of the groove). One possible explanation for the wire-like structures is superposition of the external modulation and the Al-rich bands discussed in the last paragraph.

4.5 Discussion

In some ranges of angles, the bandgap of AlGaAs exhibits a monotonic shift with respect to groove angle. This suggests that it may be possible to tune the bandgap of AlGaAs grown on a patterned substrate by varying the surface orientation.

Transmission electron micrographs of sample NSI2 show compositional modulation which intersects the substrate at an angle of 22°. While the modulation has been observed to intersect with the substrate in other grooves, this is the largest misorientation between the compositional modulation and the growth plane that we have observed. Misorientation with respect to the growth plane rules out mechanisms for orientation selective epitaxy which would produce modulation along the growth direction. This misorientation is consistent with the model proposed in section 3.

Quantum wire-like structures were observed in sample NSI3, in a groove oriented approximately along the [010] direction. The structures, which are approximately 60 Å in size, are well defined and exhibit strong contrast between the gallium and aluminum rich regions. The formation of these structures is not yet understood.

5 Conclusions

The phenomenon of orientation selective epitaxy has been introduced. We have observed the first spontaneous growth of an abrupt heterojunction lateral to the growth direction. The selective growth of OSE superlattices in grooves on a patterned substrate has been demonstrated to be a function of groove orientation. Dependence of the bandgap of AlGaAs on surface orientation presents a possible tool for bandgap engineering lateral to the growth direction. We have proposed a model for orientation selective epitaxy. Based on the model, we suggested ways to improve and modify OSE structures. The formation of facets in AlGaAs has been found to be associated with compositional variation. TEM micrographs of growth on the (211) facet show a significant misorientation of the OSE superlattice with respect to the substrate orientation, consistent with our model. Finally, we have observed quantum wire-like structures, approximately 60 Å in size, in growth on a groove oriented approximately along the [010] direction in a (100) substrate. The existence of quantum wire-like structures on this size scale, with strong, well defined variation

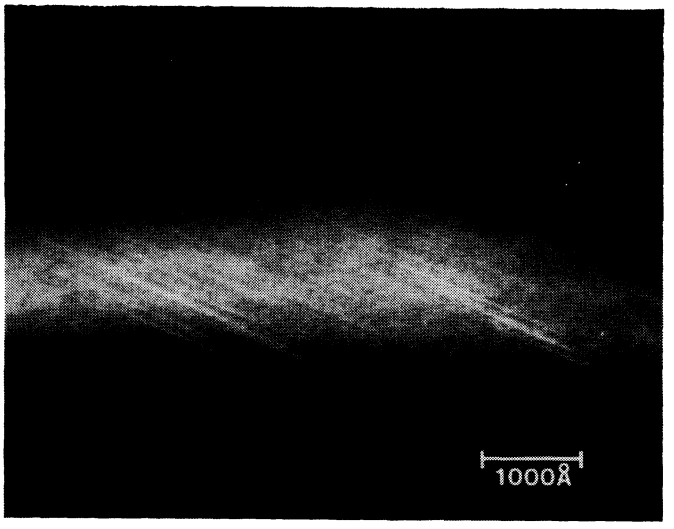

Figure 6: Transmission electron micrograph, taken using the (200)DF condition, of AlGaAs grown on the (211) facet of an [01$\bar{1}$] groove, in sample NSI2. Compositional modulation in these layers is observed to intersect the substrate at an angle of 22°. The substrate/epilayer interface contains small (111) facets, approximately 250μm in length, which are associated with an enhancement in the amplitude of the compositional modulation (see text).

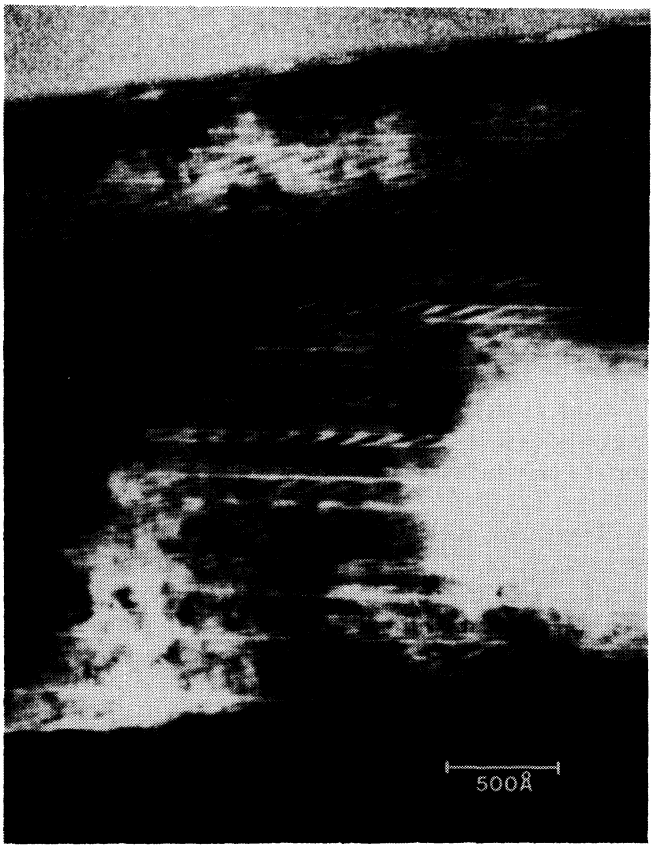

Figure 7: Transmission electron micrograph, taken using the (200)DF condition, of AlGaAs grown on the side of a [010] groove. Quantum wire-like structures are observed, with a width of approximately 60 Å.

in the aluminum concentration, suggests that orientation selective epitaxy may have applications in the fabrication of higher dimensional nanometer scale structures.

Acknowledgements

The authors wish to acknowledge C. W. Nieh, Howard Z. Chen, Hadis Morkoç, and Amnon Yariv, who were collaborators in the initial stages of this work. We are grateful to Channing Ahn and Carol Garland, for their assistance with the transmission electron microscopy. We would like to acknowledge Larry Kapitan of Northeast Semiconductor, Inc., for supplying some of the molecular beam epitaxial growths used in this work. This work was supported by the Office of Naval Research.

References

[1] Y. Arakawa, K. Vahala, and A. Yariv, Appl. Phys. Lett., **45**, 950 (1984).

[2] E. Kapon, D. M. Hwang, and R. Bhat, Phys. Rev. Lett., **63**, 430 (1989).

[3] M. Tanaka and H. Sakaki, Appl. Phys. Lett., **54**, 1326 (1989).

[4] K. Kojima, K. Mitsunaga, and K. Kyuma, Appl. Phys. Lett., **56**, 154 (1990).

[5] M. Tsuchiya, P. M. Petroff, and L. A. Coldren, Appl. Phys. Lett., **54**, 1690 (1989).

[6] Michael E. Hoenk, C. W. Nieh, Howard Z. Chen, and Kerry J. Vahala, Appl. Phys. Lett., **55**, 53 (1989).

[7] Michael E. Hoenk and Kerry J. Vahala, Rev. Sci. Instrum. **60**, 226 (1989).

[8] P. M. Petroff, J. Vac. Sci. Technol., **14**, 973 (1977).

[9] F. P. Dabkowski, P. Gavrilovic, K. Meehan, W. Stutius, J. E. Williams, M. A. Shahid, and S. Mahajan, Appl. Phys. Lett., **52**, 2142 (1988).

[10] A. Gomyo, T. Suzuki, K. Kobayashi, S. Kawata, I. Hino, and T. Yuasa, Appl. Phys. Lett., **50**, 673 (1987).

[11] W. E. Plano, D. W. Nam, J. S. Major, Jr., K. C. Hsieh, and N. Holonyak, Jr., Appl. Phys. Lett., **53**, 2537 (1988).

[12] Akiko Gomyo, Tohru Suzuki, and Sumio Iijima, Phys. Rev. Lett., **60**, 2645 (1988).

[13] H. P. Meier, E. Van Gieson, W. Walter, C. Harder, M. Krahl, and D. Bimberg, Appl. Phys. Lett., **54**, 433 (1989).

[14] P. M. Petroff, A. Y. Cho, F. K. Reinhart, A. C. Gossard, and W. Wiegman, Phys. Rev. Lett., **48**, 170 (1982).

[15] T. S. Kuan, T. F. Kuech, W. I. Wang, and E. L. Wilkie, Phys. Rev. Lett., **54**, 201 (1985).

[16] W. I. Wang, T. S. Kuan, J. C. Tsang, L. L. Chang, and L. Esaki, J. Vac. Sci. Technol. B, **4**, 517 (1986).

[17] J. M. Gaines, P. M. Petroff, H. Kroemer, R. J. Simes, R. S. Geels, and J. H. English, J. Vacuum Sci. Technol., **B6**, 1378 (1988).

[18] L. T. P. Allen, E. R. Weber, J. Washburn, Y. C. Pao, and A. G. Elliot, J. Cryst. Growth, **87**, 193 (1988).